



Contents lists available at ScienceDirect

Advanced Powder Technology

journal homepage: www.elsevier.com/locate/apt

Original Research Paper

Coarse pore evolution in dry-pressed alumina ceramics during sintering

Tsuyoshi Hondo^a, Zenji Kato^a, Kouichi Yasuda^b, Fumihiro Wakai^c, Satoshi Tanaka^{a,*}^a Department of Materials Science and Technology, Nagaoka University of Technology, 1603-1, Kamitomioka, Nagaoka, Niigata 940-2188, Japan^b Department of Materials Science and Technology, Tokyo Institute of Technology, 2-12-1-S7-14 Ookayama, Meguro, Tokyo 152-8552, Japan^c Laboratory for Materials and Structures, Tokyo Institute of Technology, R3-23 4259 Nagatsuta, Midori, Yokohama 226-8503, Japan

ARTICLE INFO

Article history:

Received 16 September 2015

Received in revised form 12 April 2016

Accepted 13 April 2016

Available online xxxxx

Keywords:

Granules

Pores

Sintering

Computed tomography

ABSTRACT

Coarse pores in a sintered ceramic often degrade its mechanical properties and reliability. In this paper, the evolution of coarse pores in a dry-pressed alumina ceramic during sintering is characterized by direct observation. Alumina compacts prepared by dry-pressing alumina powder granules were characterized using optical microscopy, electron microscopy, and micro-focus X-ray computed tomography (micro-CT) after forming and after sintering at temperatures 1300–1500 °C. Coarse pores characteristic of particle packing voids are present at granule triple points after pressing and sintering, along with remnants of the alumina granules. The coarse pores present in the powder compact grow in size and number during sintering. Coarse pore growth during sintering is attributed to the coalescence of the smaller, neighboring pores in the microstructure.

© 2016 The Society of Powder Technology Japan. Published by Elsevier B.V. and The Society of Powder Technology Japan. All rights reserved.

1. Introduction

Advanced ceramic materials are used as structural materials in a variety of applications [1]. However, widespread application of ceramics is still limited by our inability to consistently control their performance and reliability [2–8]. One of the reasons for this is the limited understanding of the origin and development of the strength and reliability limiting coarse defects. To address this issue, several methods have been developed over the years to detect coarse pores in green and sintered ceramics. Through direct observations using optical microscopy and X-ray computed tomography, the origin of coarse pores in ceramics has been identified, and the influence of coarser defects on the mechanical properties of the ceramic has been determined [2,9–13]. In particular, inhomogeneous particle-packing structures in a powder compact have been revealed using the liquid immersion (LI) method. In this method, a ceramic with a known index of refraction is immersed in a liquid of the same refractive index such that the powder compact becomes transparent due to the suppression of light scattering at the particle surfaces. The LI method makes it easy to examine the packing structure in a powder compact with an optical microscope under transmitted light [2,14–16,3]. LI

analysis has been used to image granule deformation as well as the inter- and intra-granular structure that govern the packing structure in a powder compact. Additionally, LI analysis has revealed that granule structure is retained due to binder segregation and burnout, and the interstices between remnant granules due to packing that become coarse, performance limiting defects in the green and sintered ceramic microstructure after binder burnout [17].

While the remnant granule structure explains the origin of the coarse pores in a ceramic powder compact, the evolution of coarse pore structure during sintering is still not clearly understood.

Detailed understanding of the evolution of coarse pores during sintering is required to understand and control microstructure development during sintering, and thereby control the mechanical properties and reliability of a sintered ceramic. To characterize pore evolution during sintering, ideally, the same porosity in the same sample needs to be monitored during sintering. Micro-focus X-ray computed tomography (micro-CT) is a three-dimensional (3D), non-destructive characterization tool that has recently shown great promise in the analysis of the internal pore structure of materials [18–28]. Micro-CT is expected to be a useful tool for analyzing ceramic materials as well. The objective of this study is to characterize and understand the evolution of coarse pores in an alumina powder compact during sintering using micro-CT. Microscopy analysis was also used to complement the micro-CT analysis.

* Corresponding author. Tel.: +81 258 47 9337; fax: +81 258 47 9300.

E-mail address: stanaka@vos.nagaokaut.ac.jp (S. Tanaka).

2. Experimental

2.1. Sample preparation

Industrial alumina granules (Alumina granule AKS-20, Sumitomo Chemical Co., Ltd.), which were produced by spray drying industrial alumina powder (Alumina AKP-20, Sumitomo Chemical Co., Ltd., primary particle size $\sim 0.5 \mu\text{m}$), were used in this study. Prior to forming the powder compacts, the granules were characterized using the LI method and SEM, as explained in Section 2.3. Alumina powder compacts were formed by uniaxial dry pressing the granules at 40 MPa. The powder compacts were then subjected to cold isostatic pressing (CIP) at 200 MPa (CIP, CAP50-300, NPa system Co. Ltd.). Prior to sintering at 1300–1500 °C, the powder compacts were heat-treated at 800 °C for 30 min. to remove the organic binder.

2.2. Measurement of densification behavior

The densification of the alumina powder compacts during sintering was examined. The linear shrinkage during sintering from room temperature to 1500 °C in flowing air was measured using a dilatometer (DIL 402 Expedis, NETZSCH). A cylindrical sample 6.0 mm and 9.8 mm diameter was used. The heating rate was $5 \text{ }^\circ\text{C min}^{-1}$. The bulk density of the powder compacts was measured from the sample dimensions and weight after sintering at 1300, 1400, and 1500 °C in an ambient atmosphere. The relative density was calculated from the bulk density and the ultimate density of alumina 3.99 g cm^{-3} .

2.3. Characterization of granules and compact structure

(1) LI analysis

The internal structure of the granules and the powder compacts was characterized using the LI method. The powder compact was chopped to approximately 500 μm thick and polished to approximately 100 μm thick using sandpaper. Matching index of refraction liquids methylene iodide and bromonaphthalene were used as the immersion liquids for the granules and the powder compacts, respectively [5–7]. The internal structure of the granules and the powder compact was observed using an optical microscope (DX-51, OLYMPUS Corp.) with transmitted light, both before and after binder burnout.

(2) Micro-CT analysis

The evolution of the coarse pore structure within an alumina compact during sintering from 1300 to 1500 °C was observed using micro-CT (SkyScan 1172, BRUKER AXS). Samples for analysis were prepared by cutting an alumina compact into $1 \text{ mm} \times 1 \text{ mm} \times 1 \text{ mm}$ cubes. The alumina compact structure was characterized after sintering at 1300, 1400, and 1500 °C in an ambient atmosphere. For sintering, the heating rate was $5 \text{ }^\circ\text{C/min}$, the duration at the peak temperature was 0 min, and the cooling rate was $10 \text{ }^\circ\text{C/min}$. After sintering at each of these temperatures, the sample was characterized using micro-CT, and then placed back into the furnace to continue sintering. Internal pores larger than $\sim 5 \mu\text{m}$ were characterized using micro-CT with a voltage of 40–100 kV, a current of 100–250 μA , and a rotation angle of 0.1° . The image data obtained were analyzed using 2D/3D software (SkyScan, CTAn).

(3) SEM analysis

The granules were characterized using SEM (JEOL, JSM-5310LV). Size distribution of granules were measured from SEM images. The

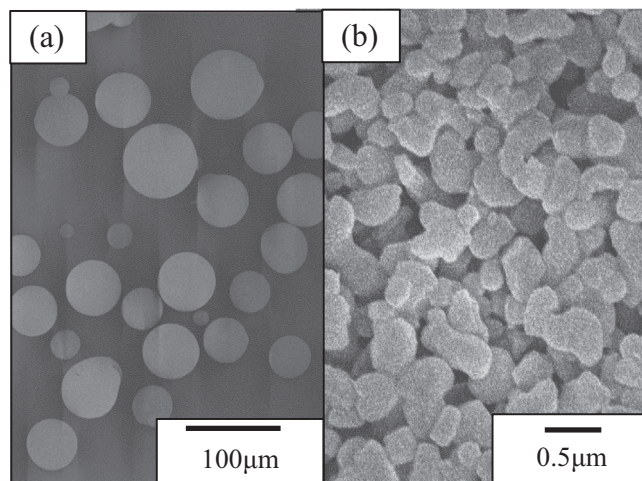


Fig. 1. SEM micrograph of alumina granules used in this study. (a) Spherical morphology alumina granules; (b) primary particles within the alumina granules.

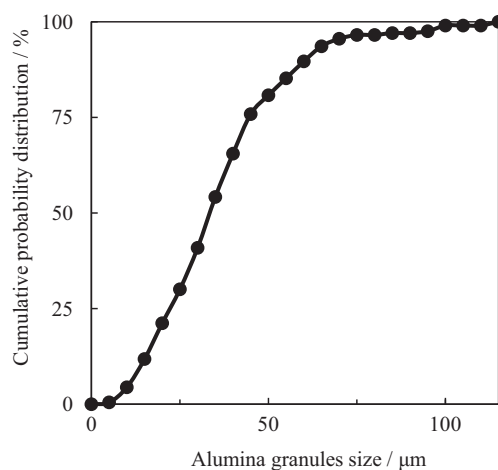


Fig. 2. Size distribution of alumina granules.

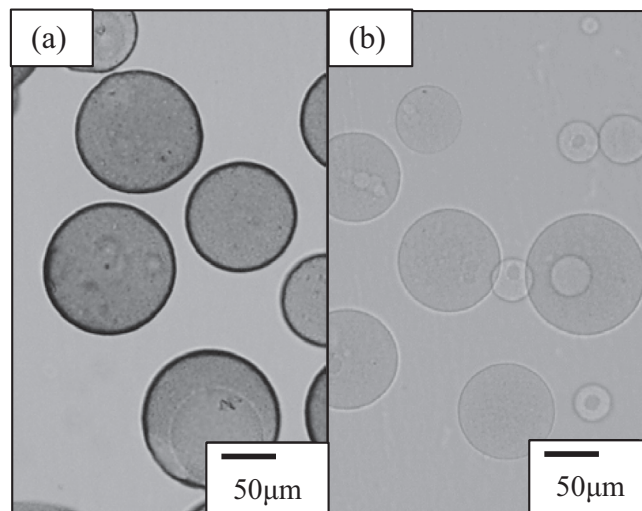


Fig. 3. Optical micrograph of alumina granules characterized using the LI technique. (a) Before binder burnout, showing binder migration to the granule surface. (b) After binder burnout, showing large internal cavities (darker spots).

Download English Version:

<https://daneshyari.com/en/article/10260368>

Download Persian Version:

<https://daneshyari.com/article/10260368>

[Daneshyari.com](https://daneshyari.com)